

Paused Pol II Coordinates Tissue Morphogenesis in the *Drosophila* Embryo

Mounia Lagha,^{1,5} Jacques P. Bothma,^{2,5} Emilia Esposito,¹ Samuel Ng,¹ Laura Stefanik,³ Chiahao Tsui,¹ Jeffrey Johnston,⁴ Kai Chen,⁴ David S. Gilmour,³ Julia Zeitlinger,⁴ and Michael S. Levine^{1,*}

¹Department of Molecular and Cell Biology

²Biophysics Graduate Group

University of California, Berkeley, Berkeley, CA 94720, USA

³Center for Gene Regulation, Department of Biochemistry and Molecular Biology, The Pennsylvania State University, University Park, PA 16802, USA

⁴Stowers Institute for Medical Research, Kansas City, MO 64110, USA

⁵These authors contributed equally to this work

*Correspondence: mlevine@berkeley.edu

<http://dx.doi.org/10.1016/j.cell.2013.04.045>

SUMMARY

Paused RNA polymerase (Pol II) is a pervasive feature of *Drosophila* embryos and mammalian stem cells, but its role in development is uncertain. Here, we demonstrate that a spectrum of paused Pol II determines the “time to synchrony”—the time required to achieve coordinated gene expression across the cells of a tissue. To determine whether synchronous patterns of gene activation are significant in development, we manipulated the timing of *snail* expression, which controls the coordinated invagination of ~1,000 mesoderm cells during gastrulation. Replacement of the strongly paused *snail* promoter with moderately paused or non-paused promoters causes stochastic activation of *snail* expression and increased variability of mesoderm invagination. Computational modeling of the dorsal-ventral patterning network recapitulates these variable and bistable gastrulation profiles and emphasizes the importance of timing of gene activation in development. We conclude that paused Pol II and transcriptional synchrony are essential for coordinating cell behavior during morphogenesis.

INTRODUCTION

The early *Drosophila* embryo is the premier system for visualizing gene activity in animal development. In a period of just 1 hr, broadly distributed maternal determinants generate localized patterns of gene activity, including segmentation stripes of gene expression (Chen et al., 2012). A variety of studies suggest that enhancers, typically 300–500 bp in length, are responsible for determining where and when developmental control genes are switched on and off (Ong and Corces, 2011). With few excep-

tions, localized patterns of expression can be attributed to discrete enhancers located upstream, downstream, or within the gene of interest.

The enhancer is therefore seen as the key agent of differential gene activity in animal development (Ong and Corces, 2011). Considerably less is known about the role of the promoter in the regulation of the spatial or temporal limits of gene expression, although they are known to control the rates of RNA synthesis (Juven-Gershon and Kadonaga, 2010). In the simplest view, enhancers determine the limits of gene expression (where and when genes are active), whereas the promoter controls the levels of expression (e.g., how many transcripts are produced in a given unit of time).

The purpose of this study is to determine whether the promoter regions of developmental control genes can influence the timing or spatial limits of gene expression in the early *Drosophila* embryo. We were motivated by the recent finding that many developmental control genes contain paused RNA polymerase (Pol II) prior to their activation during embryogenesis (Adelman and Lis, 2012; Levine, 2011). The function of paused Pol II is uncertain, despite its apparent prevalence (~30% of all protein coding and noncoding genes) in both *Drosophila* embryos and mammalian stem cells (Guenther and Young, 2012).

The prototypic example of paused Pol II, *Drosophila* heat shock genes, underlies rapid induction of gene expression in response to stress (Boehm et al., 2003). There is also evidence that paused Pol II serves to keep promoters “open” by excluding or diminishing the occurrence of positioned nucleosomes that occlude the transcription start site in cultured cells (Gilchrist et al., 2010). Recent quantitative imaging methods suggest that paused Pol II influences synchronous induction of gene expression across the different cells of presumptive tissues in the early *Drosophila* embryo (Boettiger and Levine, 2009).

In the latter study, quantitative in situ hybridization assays were used to detect the first nascent transcripts encoded by different developmental control genes, within the first 10–20 min after the onset of expression in precellular embryos,

~2 hr after fertilization. Genes were classified as synchronous if nascent transcripts were detected in over 50% of the nuclei that will eventually express a given gene or stochastic if expressed in fewer than 50%. Most paused genes exhibited synchronous patterns of activation, whereas most nonpaused genes displayed stochastic expression. The evidence linking paused polymerase and synchrony was strictly correlative, and there is no evidence that these modes of activation are significant in development.

Here, we employ quantitative imaging (Bothma et al., 2011; Perry et al., 2010), whole-genome Pol II-binding assays (Zeitlinger et al., 2007), and BAC transgenesis (Venken et al., 2006) to examine the function of paused Pol II in the early *Drosophila* embryo. Evidence is presented that minimal promoter sequences, ~100–200 bp centered around the +1 transcription start site, are sufficient for establishing paused Pol II and mediating rapid, synchronous activation of gene expression in transgenic embryos. Those genes containing high levels of paused Pol II achieve coordinate expression more rapidly than those containing low levels.

To determine whether the “time to synchrony” is important in development, we manipulated the coordinate expression of *snail* (*sna*) (*Slug/Sna2* in vertebrates), a major determinant of epithelial-mesenchyme transitions (EMTs) in animal development. In *Drosophila*, *sna* is expressed in ~1,000 cells comprising the presumptive mesoderm (Kosman et al., 1991; Leptin and Grunewald, 1990). These cells undergo coordinated invagination during gastrulation, within 90 min of the onset of *sna* expression (Leptin, 2005; Sweeton et al., 1991). To determine whether synchronous activation of *sna* expression is essential for coordinated invagination of the mesoderm, we replaced the native *sna* promoter with those from moderately paused (*short gastrulation*; *Chordin*) or nonpaused (*thisbe*; *Fgf8*) genes. These heterologous promoters result in less synchronous patterns of *sna* activation and a progressive reduction in mesoderm invagination during gastrulation. We therefore conclude that paused Pol II and transcriptional synchrony are essential for coordinating cell behavior during morphogenesis.

RESULTS

Previous studies suggested a correlation between paused Pol II and synchronous patterns of gene activation in the *Drosophila* embryo. Moreover, computational analyses identified sequence elements that are associated with promoters containing paused Pol II, including GAGA and pause button (PB) motifs (e.g., Gilchrist et al., 2010; Hendrix et al., 2008; Lee et al., 2008; Shopland et al., 1995). These observations raise the possibility that the core promoter might be sufficient to determine whether a gene is paused or not paused and activated in a synchronous or stochastic fashion.

As a first step toward testing this possibility, we examined the regulation of two Dpp (BMP) target genes, *pannier* (*pnr*; *GATA4*) and *tailup* (*tup*; *Islet-1*), transcription factors essential for the specification of a variety of dorsal tissues, including the heart (Vincent and Buckingham, 2010). These genes are coactivated in the dorsal ectoderm of 2 hr embryos (e.g., Ashe et al., 2000) but, nonetheless, display opposite Pol II-binding profiles. *tup* is strongly paused, whereas *pnr* lacks Pol II (Zeitlinger et al.,

2007). The use of quantitative imaging methods revealed differences in their activation profiles that were missed in previous studies, as discussed below (Figure 1).

Temporal Coordination of Dpp Target Genes

tup is activated by high levels of the Dpp gradient, whereas *pnr* is triggered by low levels (Figures 1A–1H) (Ashe et al., 2000). These distinctive spatial expression patterns depend on previously identified *tup* and *pnr* enhancers. Quantitative imaging methods reveal that they also exhibit dissimilar temporal profiles (Figures 1E–1I).

It was previously shown that *tup* contains paused Pol II and is activated in a synchronous fashion, whereas *pnr* lacks Pol II and exhibits stochastic expression (Boettiger and Levine, 2009). We developed high-resolution confocal visualization and image segmentation methods to measure the time to synchrony, i.e., the degree of temporal coordination in gene activation during nuclear cleavage cycle (cc) 14, the 1 hr interval preceding gastrulation (Figures 1A–1H). The ~6,000 cells comprising the pregastrula embryo are synchronized within the cell cycle, thereby permitting direct comparisons of transcriptional coordination. Quantitative FISH assays permit detection of nascent transcripts shortly after the onset of gene expression (e.g., Bothma et al., 2011). In this assay, activation is defined as the time it takes for 50% of the nuclei to express nascent transcripts (t50). Using a cumulative gamma distribution, we fit a curve to each experimental data set (see Figure S1 available online; Supplemental Information). t50 values are calculated by measuring the fraction of nuclei that express a given gene for each fitted activation profile. Pregastrula cc14 embryos are selected based on nuclear density and embryo morphology and then ordered relative to one another based on the fraction of the expression pattern containing nascent transcripts. The collections are designed to ensure that embryos are distributed in an unbiased way across the entirety of cc14. This approach allows us to measure the t50 values with an accuracy of ± 5 min (see Table 1; Figure S1; Table S1; Supplemental Information).

The endogenous *tup* and *pnr* genes exhibit distinct t50 activation profiles: *tup* achieves t50 expression ~26 min after the onset of cc14, whereas *pnr* does not exhibit comparable expression for another 15 min (Table 1). This represents a significant delay because the entire cc14 interphase extends for just 55 min (see below). To determine whether these divergent temporal expression profiles are due to enhancer or promoter sequences, we created a BAC transgene encompassing the entire *tup* transcription unit and flanking regulatory DNAs that recapitulates the rapid and synchronous activation profile of the endogenous *tup* locus (Figures 1J and S2). In these experiments, the *tup* transcription unit was replaced with the *yellow* reporter gene to facilitate detection of nascent transcripts (Perry et al., 2010). There is a slight delay in the t50 value of the BAC transgene (~32 min) as compared with the endogenous *tup* locus (~26 min) (Table 1), which is likely due to the heterologous site of transgene insertion, a slower rate of *yellow* transcription, or the use of heterozygous embryos to measure expression of BAC transgenes (see Figures 1I and 1J).

We next examined the activation profile obtained upon replacement of the paused *tup* promoter (*tupPr*) with the

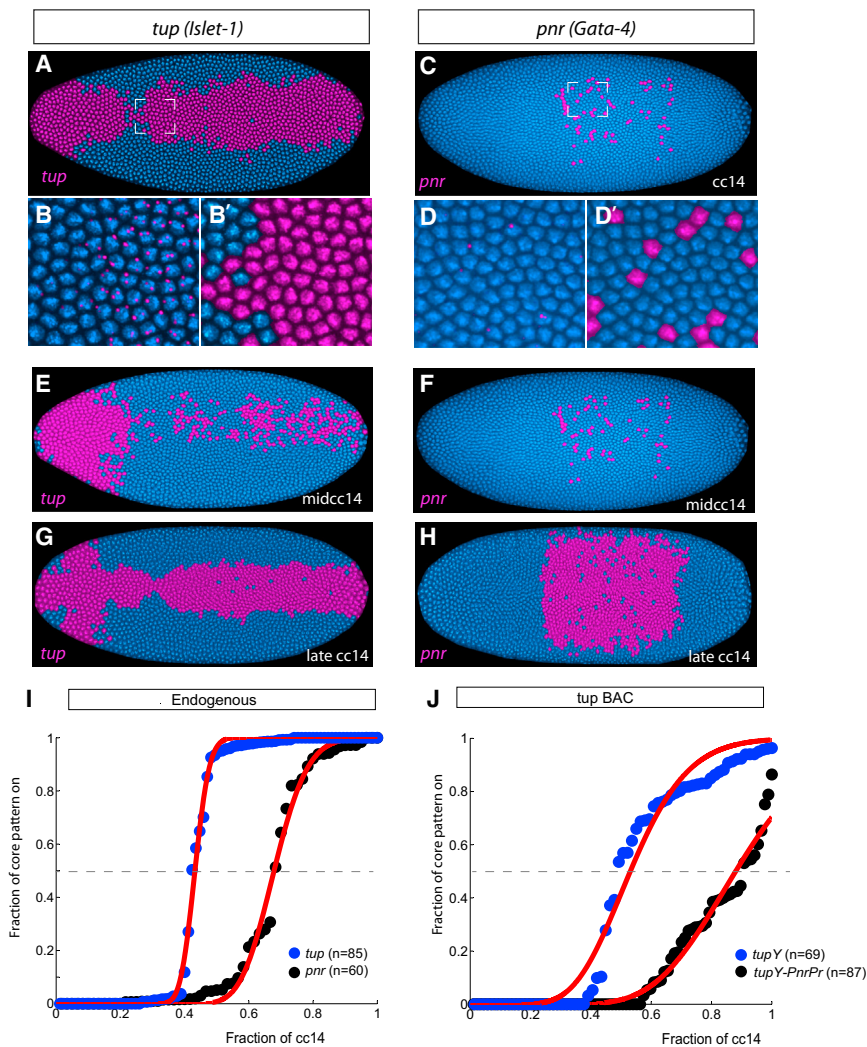


Figure 1. BMP/Dpp Target Genes Exhibit Distinct Coordination Profiles

(A–H) cc14 embryos hybridized with *tup* and *pnr* fluorescent (magenta) intronic probes for detecting nascent transcripts (nuclei stained with DAPI [blue]). Raw images for *tup* and *pnr* transcripts are shown in (B) and (D), and the corresponding processed images are shown in (B') and (D'). Images shown in (B) and (D) are magnifications of bracketed regions in (A) and (C). (E–H) *tup* (E and G) and *pnr* (F and H) expression during mid (E and F) and late (G and H) cc14.

(I and J) Dynamics of gene expression during cc14 based on the fraction of nuclei containing nascent transcripts. (I) Endogenous *tup* expression (blue) reaches 50% of the complete pattern (t50, 26) 15 min earlier than does *pnr* (black) (t50, 41). (J) There is a delay in *tup* dynamics when the minimal promoter of a *tup* BAC transgene (*tupY*) is replaced by that of *pnr* (*tupY-PnrPr*) (see also Figure S2). The red curves represent the fitted curves (using a cumulative gamma distribution) to the data depicted in (I) and (J) (see Supplemental Information; Figure S1; Table S1). t50 values are determined from these fitted curves.

Minimal Promoter Sequences Are Sufficient to Establish Paused Pol II

The preceding results suggest that minimal promoter sequences might be sufficient to determine whether a gene is activated in a synchronous or stochastic fashion. To establish whether they are also sufficient for determining the presence or absence of paused Pol II, we analyzed minigenes containing the *pnr* intronic enhancer (*pnrE*), *tupPr*, and *yellow* reporter gene (*pnrE > tupPr/yellow*). This minigene exhibits synchronous expres-

sion in the dorsal ectoderm of wild-type embryos (see below) but is inactive in *Toll^{10b}* mutants due to the absence of Dpp signaling (Schneider et al., 1991). Both the endogenous *tup* locus and the minigene nonetheless contain paused Pol II in these “silent” *Toll^{10b}* embryos (Figures 2A and 2B); as expected, the endogenous *pnr* locus lacks paused Pol II (Zeitlinger et al., 2007) (Table S2). Permanganate footprint assays identified hypersensitive thymidine residues at positions +48 and +51 nucleotides downstream of the *tup* transcription start site in transgenic embryos (Figure 2C), strengthening the evidence that the stalled Pol II identified at the *tupPr* represents promoter-proximal paused Pol II.

Thus, the 200 bp *tupPr* region is sufficient for the establishment of paused Pol II (and synchronous expression, as shown below). It contains key signatures of paused promoters (Gilchrist et al., 2010; Hendrix et al., 2008; Lee et al., 2008; Shopland et al., 1995), including 5' GAGA elements located ~100 bp upstream of the transcription start site, and PB motifs positioned +54 to +64 bp downstream of the start site, in the vicinity of the hypersensitive thymidine residues identified by permanganate

nonpaused *pnr* promoter (Figures 1J and S2). The modified BAC transgene is identical to the control, except for the substitution of just 200 bp centered around the +1 transcription start site of the *pnr* promoter (Figure S3). The modified transgene was inserted into the same chromosomal location as the control transgene, thereby permitting direct quantitative comparisons of their activation dynamics. Surprisingly, this 200 bp substitution within the large 60 kb BAC transgene is sufficient to convert the rapid and synchronous *tup*-*yellow* expression pattern into a slow and stochastic mode of activation (Figure 1J).

The modified transgene exhibits a t50 value of 53 min, which is considerably slower than the t50 values seen for the endogenous *tup* locus (26 min) or unmodified *tup* BAC transgene (32 min). It is somewhat slower than the t50 value seen for the endogenous *pnr* locus (41 min), although the differential timing of the *tup* versus *pnr* promoters (Δ t50) is similar for the endogenous loci and BAC transgenes, at 15 and 21 min, respectively (Table 1). These findings suggest that the *pnr* promoter, not enhancers, is the prime determinant of its slow and stochastic activation profile during development.

Table 1. Summary of the t50 Values for All of the Constructs Used in This Study

Promoter	t50 Time (min)	Uncertainty from Simulations (min)
PnrPr Endo	41	3
TupPr Endo	26	3
Tup-Y BAC	32	3
Tup-Y-PnrPr BAC	53	2
PnrE-TupPr NelfE/Spt5	39	4
PnrE-TupPrShort	31	3
PnrE-TupPr Trl	30	4
PnrE-TupPr	15	3
PnrE-SnaPr	24	3
PnrE-Hsp70Pr	28	4
PnrE-SogPr	38	4
PnrE-ThsPr	55	2
PnrE-PnrPr	74	4
SnaE-SnaPr	3	2
SnaE-SogPr	22	4
SnaE-ThsPr	40	3
SnaE-PnrPr	42	3
SogE-TupPr	1	0.6
SogE-SnaPr	1	0.6
SogE-PnrPr	35	7

t50 corresponds to the time it takes for an embryo to show nascent transcription in 50% of the pattern. t50 is an estimated time based on the measured activated kinetics of many embryos (see also Figure S1 and Table S1).

protection assays (Figures 2C and S3). We therefore conclude that minimal promoter sequences are sufficient to establish paused Pol II in vivo, in the *Drosophila* embryo. In principle, any gene can be artificially “paused” or “depaused” by exchanging minimal promoter sequences. Such an approach may be relevant to the stem cell field because some of the key determinants of pluripotency (e.g., Nanog) exhibit stochastic expression among the different ICM cells of mouse embryos (Kalmar et al., 2009; Nichols and Smith, 2011).

Promoter-Associated Elements Influence Transcriptional Synchrony

To establish a sharper connection between “pausing elements” in the *tupPr* and transcriptional synchrony, we expressed the *pnrE > tupPr/yellow* transgene in embryos containing diminished levels of the GAGA-binding protein, GAF (or Trl). Previous studies implicated GAGA and Trl in the stable association of paused Pol II within the proximal promoter of *Hsp70* (Fay et al., 2011; Lee et al., 1992; Shopland et al., 1995). The *tupPr* region contains GAGA elements located ~100 bp upstream of the transcription start site (Figure S3), and whole-genome assays confirm GAF/Trl binding to this region in the *Drosophila* embryo (Schuettengruber et al., 2009). Reduced levels of Trl caused an ~20 min delay in the activation of the *pnrE > tupPr/yellow* transgene, as compared with wild-type embryos

(Figure 2D; Table1), similar to the activation profile mediated by the nonpaused *thisbe* promoter (see below). An equivalent delay is observed with a truncated *tupPr* lacking upstream GAGA elements but retaining all core elements such as the INR (Figure 2D; Table1). These studies suggest a close correlation between Trl/GAGA and the temporal coordination of gene activation.

The stability of paused Pol II also depends on negative elongation factors, such as NELF and Spt5, which bind nascent transcripts shortly after the onset of transcription (Gilchrist et al., 2010; Li and Gilmour, 2011). There is an ~30 min delay in the activation profile of the *pnrE > tupPr/yellow* transgene in embryos containing reduced levels of NelfE and Spt5 (Figure 2D; Table1). Thus, the preceding findings suggest a close correlation among minimal promoter sequences, paused Pol II, and the time to synchrony in the *Drosophila* embryo.

A Spectrum of Synchrony

Whole-genome Pol II chromatin immunoprecipitation sequencing (ChIP-seq) assays suggest that genes might not be simply paused or nonpaused, and activated in a strictly synchronous or stochastic fashion. Instead, there are different levels of Pol II in the promoter regions of genes previously identified as stalled or not stalled (Figure 3F; see Zeitlinger et al., 2007). Normalized levels of paused Pol II were measured in vivo in dorsal-ventral patterning mutants containing a single embryonic tissue, in which the gene in question is silent (Figure 3F). For example, *tup* is not expressed in *Toll^{10b}* mutant embryos because they contain only mesoderm due to the transformation of ectoderm into mesoderm. Conversely, *sna* is not expressed in *gd⁷* mutant embryos, which display the reciprocal transformation of mesoderm into ectoderm. The *tup* and *sna* promoters contain significantly more Pol II sequence reads than *sog* in silent mutant embryos, even though all three genes were classified as stalled or paused in previous studies (Zeitlinger et al., 2007). Similarly, *thisbe* contains more Pol II than *pnr*, even though both genes were classified as nonstalled. *tup* is consistently seen to contain the highest levels of promoter-proximal Pol II read counts in a variety of tissues (Gaertner et al., 2012).

To investigate the significance of these different levels of Pol II, we analyzed the expression of a series of minigenes containing the *pnr* enhancer (*pnrE*) and six different promoter sequences encompassing a spectrum of paused Pol II (Figure S3). Remarkably, the activation profiles of these minigenes mirror the levels of Pol II binding (Figure 3E; Table 1). The *tupPr* contains the highest levels of Pol II and exhibits a t50 value of just ~15 min. This is followed by progressively slower profiles for *sna* (t50, 24 min), *hsp70* (28 min), and *sog* (38 min), which contain successively lower levels of Pol II.

Finally, the promoter regions of the nonpaused genes *ths* and *pnr* exhibit the slowest activation dynamics, although *ths* is somewhat faster (t50, 55 min) than *pnr* (t50, 74 min). A similar correlation between the levels of paused Pol II and the time to synchrony was seen for minigenes containing the *sog* intronic enhancer, which mediates activation in the neurogenic ectoderm (Figures S4A–S4D; Table1), and for the distal *sna* enhancer (*snaE*) in the mesoderm (see below).

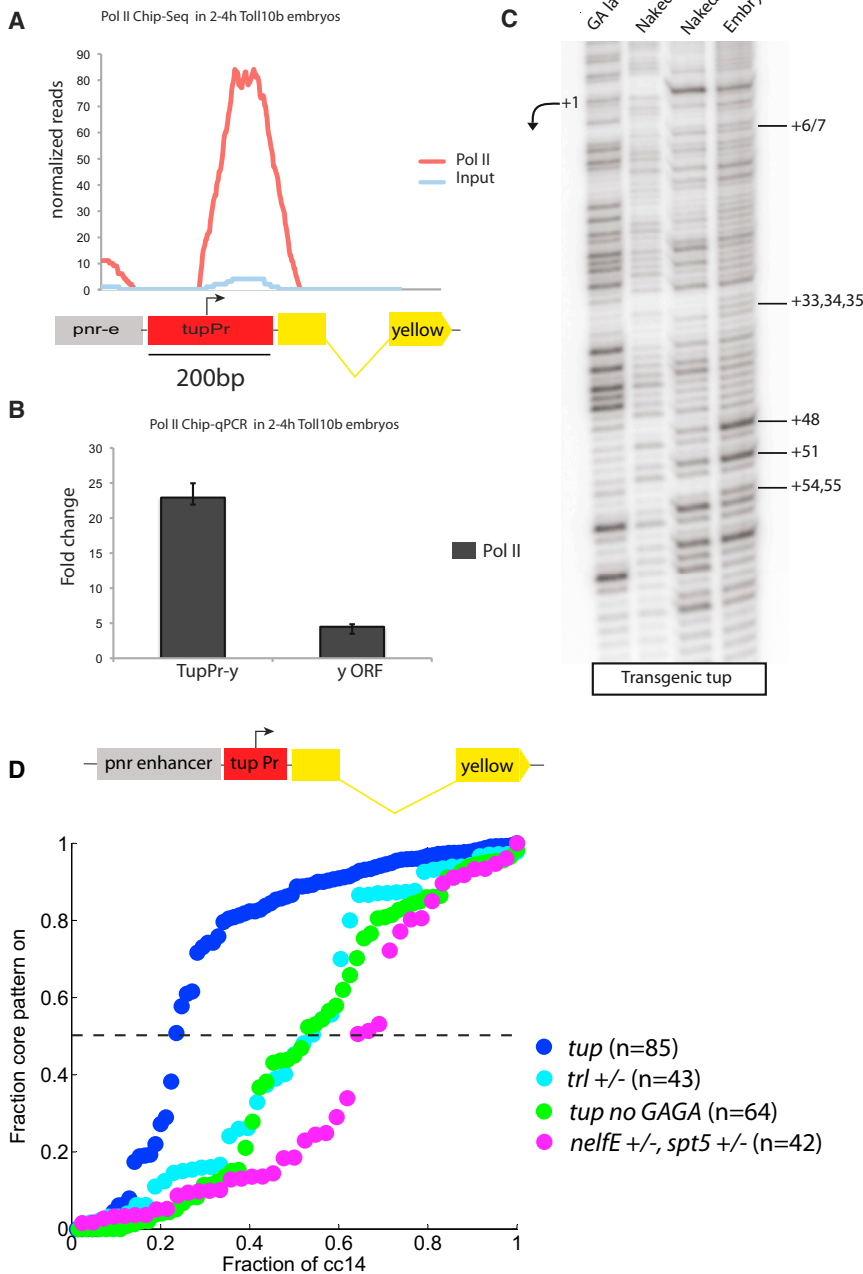


Figure 2. The Minimal Promoter Mediates Paused Pol II

(A) Pol II ChIP-seq reads of the *pnr/tup* transgene in a tissue where it is silent. (B) Pol II ChIP followed by qPCR showing enrichment at the *tupPr/yellow* junction. y ORF, yellow open reading frame. Error bars represent SD. (C) Permanganate footprinting reveals a promoter-proximal “transcription bubble” in mutant embryos where the *tupPr/yellow* transgene is silent. (D) Reduced levels of maternal *Trl* (turquoise) or *NelfE/Spt5* (pink) cause a delay in the expression profile of the *pnrE > tupPr* transgene. A similar effect is observed with a truncated version of the *tupPr* lacking the upstream GAGA sites. See also Figure S3 for relevant promoter sequences.

exhibits a 19 min delay in the t50 profile (Figure 4D; Table 1). As expected, the nonpaused *ths* and *pnr* promoters mediate even slower activation profiles (t50, 40 and 42 min, respectively). The *snaE* mediates more rapid onset of expression in cc14 than the *pnrE*, probably due to the earlier availability of activators (e.g., Dorsal and Twist) in the mesoderm as compared with the dorsal ectoderm (e.g., pSmad). Nonetheless, after upstream activators initiate expression, the detailed temporal dynamics (t50 activation) are determined by the different promoter sequences.

The *sna*, *sog*, and *ths* promoters provide a nice spectrum of activation during cc14 (t50 values of 3, 22, and 40 min, respectively) and seem ideally suited for manipulating the synchrony of *sna* expression in the presumptive mesoderm. Our choice of *sna* stems from the short lag time, less than 90 min, between the onset of transcription and morphogenesis—the coordinate invagination of the ventral mesoderm during gastrulation (see below). However, the accurate interpretation of any changes in gastrulation arising from the use of

Transcriptional Synchrony and Rates of RNA Synthesis

The preceding findings demonstrate that the same enhancer can produce a spectrum of activation profiles in the ectoderm of early embryos. To determine the feasibility of manipulating the timing of gene expression in the presumptive mesoderm, we placed the distal (shadow) *snaE* (Dunipace et al., 2011; Perry et al., 2010) upstream of the *sna*, *sog*, *ths*, and *pnr* promoters and *yellow* reporter gene (Figures 4A–4C). We observed similar relative t50 values as those obtained with the *pnrE* (Figure 3; Table 1). The *sna* promoter mediates a t50 value of 3 min, whereas the more weakly paused *sog* promoter

heterologous promoters requires an understanding of the relationship between t50 activation profiles and the levels of gene expression.

We expected promoters mediating slow synchrony profiles (e.g., *ths*) to produce weaker expression than those mediating rapid synchrony (e.g., *sna* promoter). Single-molecule in situ hybridization (smFISH) assays (Boettiger and Levine, 2013) were employed to measure the number of *yellow* mRNAs produced by different yellow minigenes: *snaE > pnrPr/yellow*, *snaE > thsPr/yellow*, and *snaE > snaPr/yellow* (Figure 4E). As expected, the “slow” minigenes produce lower levels of *yellow* mRNAs

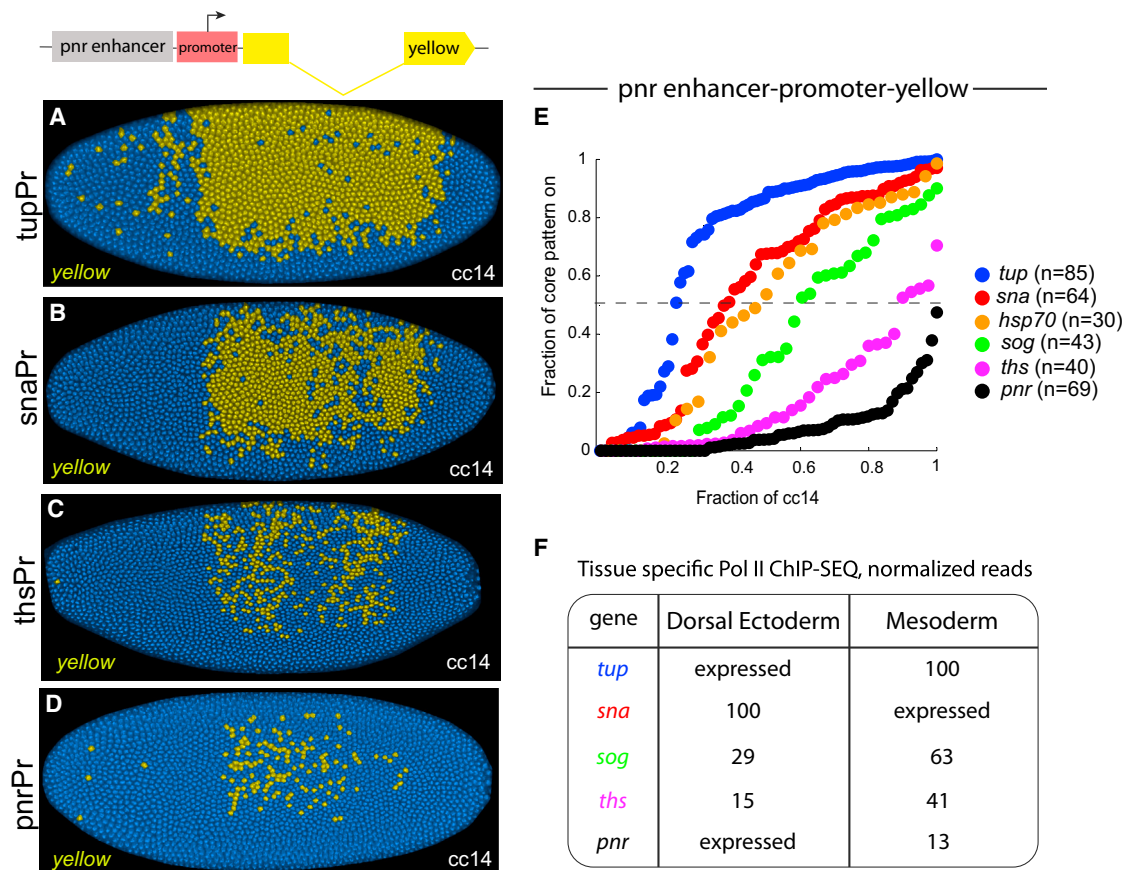


Figure 3. A Spectrum of Synchrony

The *pnrE* was placed upstream of the *tup*, *sna*, *Hsp70*, *sog*, *ths*, and *pnr* promoters (Pr) (see diagram in upper left).

(A–D) Examples of transgenic embryos stained with a *yellow* intronic probe at the midpoint of *cc14*. The *tupPr* mediates synchronous expression in the dorsal ectoderm (A), whereas the *pnrPr* mediates stochastic expression (D).

(E) Temporal coordination profiles during *cc14*. The *tupPr* provides the rapid coordination profile, whereas the *pnr* promoter exhibits the slowest coordination. *Sog* and *ths* give intermediate.

(F) Relative amounts of Pol II at the promoter regions of inactive genes. For actively expressed genes, we denote them as “expressed”; the normalized Pol II reads are provided in Table S2.

than the “fast” genes. The *pnr*, *ths*, and *sna* promoters produce 30 ± 10 , 60 ± 20 , and 100 ± 30 mRNAs per cell, respectively, in the mesoderm prior to invagination.

Modeling methods were used to estimate promoter strength based on activation kinetics (see Supplemental Information; Figures S4E–S4I). The different levels of *yellow* mRNAs produced by the *ths* and *sna* promoters can be attributed to their respective t50 activation profiles. The *snaE* > *thsPr*/*yellow* mini-gene is expressed at lower levels than *snaE* > *snaPr*/*yellow* due to its slower synchrony profile. However, once activated in a given cell, the *ths* promoter appears to mediate a similar rate of RNA synthesis as the *sna* promoter (see Supplemental Information; Figures S4E–S4I). Similarly, quantitative measurements suggest that the *sog* promoter mediates a similar rate of expression as the *sna* and *ths* promoters once activated (see below). In contrast, the low levels of *yellow* mRNAs produced by the *pnr* promoter probably result from the combination of a slow synchrony profile and a lower rate of RNA synthesis. Thus, we focused on the use of the *ths* and *sog* promoters to

examine the consequences of “desynchronizing” the onset of *sna* expression.

Transcriptional Synchrony Is Essential for Coordinate Invagination

A 25 kb *sna* BAC transgene encompassing the *sna* transcription unit, proximal enhancer, and neighboring *Tim17B2* locus (which harbors the distal *sna* shadow enhancer) was shown to be sufficient to rescue the gastrulation defects of *sna*⁻¹/*sna*⁻ mutant embryos (Dunipace et al., 2011; Perry et al., 2010). However, there is evidence that the proximal enhancer might attenuate *sna* expression by impeding access of the distal enhancer to the *sna* promoter (Dunipace et al., 2011) (data not shown). Consequently, we removed this enhancer in order to obtain a more direct assessment of the contributions of the different promoters in coordinating mesoderm invagination. It is important to note that the distal enhancer is sufficient for complete rescue of the gastrulation defects of *sna*⁻¹/*sna*⁻ mutant embryos and the development of fully viable adult flies (Dunipace et al., 2011).

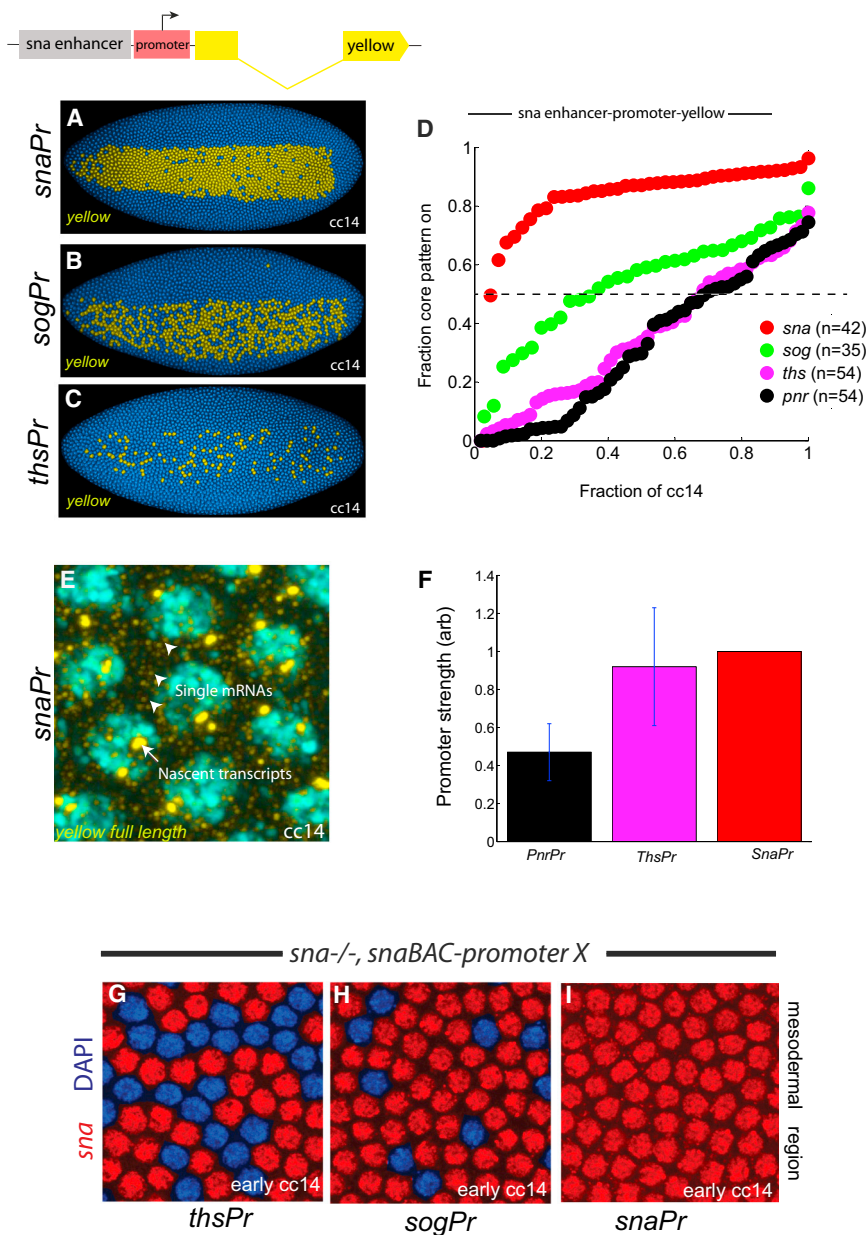


Figure 4. Minimal Promoters Are Sufficient to Perturb *sna* Temporal Coordination

The distal *snaE* was placed upstream of the *snaPr* (A), *sogPr* (B), and *thsPr* (C) promoters attached to the *yellow* reporter gene (see diagram in upper left).

(A–C) Processed images after FISH using a *yellow* intronic probe.

(D) Temporal coordination profiles during cc14.

(E) High-resolution confocal image of *yellow* mRNAs encoded by the *snaE* > *snaPr*/*yellow* minigene. Arrowheads point to individual cytoplasmic mRNAs; arrow indicates nascent transcripts.

(F) Bar graph showing the estimated promoter strength from the *pnr*, *ths*, and *sna* promoters just prior to gastrulation (see [Experimental Procedures](#) and [Figure S4](#)). Error bars represent SD. a.u., arbitrary units.

(G–I) False-colored nuclei showing the presence of nascent transcripts for *sna* in the rescue BAC constructs containing the *ths* (G), *sog* (H), and *sna* (I) promoter.

([Figures 5A–5D](#)). In contrast, the transgene containing the moderately paused *sog* promoter produces truncated furrows ([Figures 5E, 5F, and 5H](#)) (18 out of 22) but occasionally induces nearly complete furrows approaching those seen in wild-type embryos ([Figures 5G and 5G'](#)) (4 out of 22). Finally, the nonpaused *ths* promoter produces highly variable phenotypes, ranging from the complete absence of invagination (11 out of 16), to erratic pockets of ingressing cells (3 out of 16) ([Figures 5I and 5J](#)), and rarely, extended grooves of invaginating cells (2 out of 16) ([Figures 5K and 5K'](#)). Snail mRNAs and protein are detected only in the invaginating cells of partially rescued embryos exhibiting truncated furrows or isolated pockets of ingression ([Figures 5D, 5H, 5L, and S5A–S5F](#)). These studies suggest that the time to synchrony is a

We employed recombining methods to create a series of *sna* BAC transgenes that contain either *sog* or *ths* promoter sequences in place of the native *sna* promoter (replacement of ~100–110 bp; see [Figure S3](#)). The three BAC transgenes (native *sna* promoter, *sog* promoter, or *ths* promoter) exhibit distinctive patterns of activation during the onset of cc14 ([Figures 4G–4I](#)), concomitant with the levels of paused Pol II and the t50 synchrony values seen for the *sna* minigenes ([Figures 4A–4D](#)).

There is a tight correlation between these activation profiles and the extent to which mesoderm invagination is rescued in *sna*⁻/*sna*⁻ embryos ([Figure 5](#)). Thus, the “native” transgene containing the strongly paused *sna* promoter mediates a coordinated ventral furrow and robust invagination of the mesoderm

critical determinant of coordinate cell behavior in development (see below).

Computational Models of Gastrulation Variability

We constructed a mathematical model ([Figures 6A–6C](#)) to explain the highly variable gastrulation phenotypes seen for the *sna* BAC transgenes containing the *sog* and *ths* promoters. Bistability of *sna* expression is often observed in the anterior third of the embryo encompassing ~300 of the ~1,000 cells comprising the ventral furrow (e.g., [Figures 5E', 5F', and 5K'](#)). This model makes use of the wealth of knowledge about the transcription networks governing the dorsal-ventral patterning of the *Drosophila* embryo (reviewed by [Rushlow and Shvartsman, 2012](#)). It also draws on recent dynamic imaging of the Dorsal

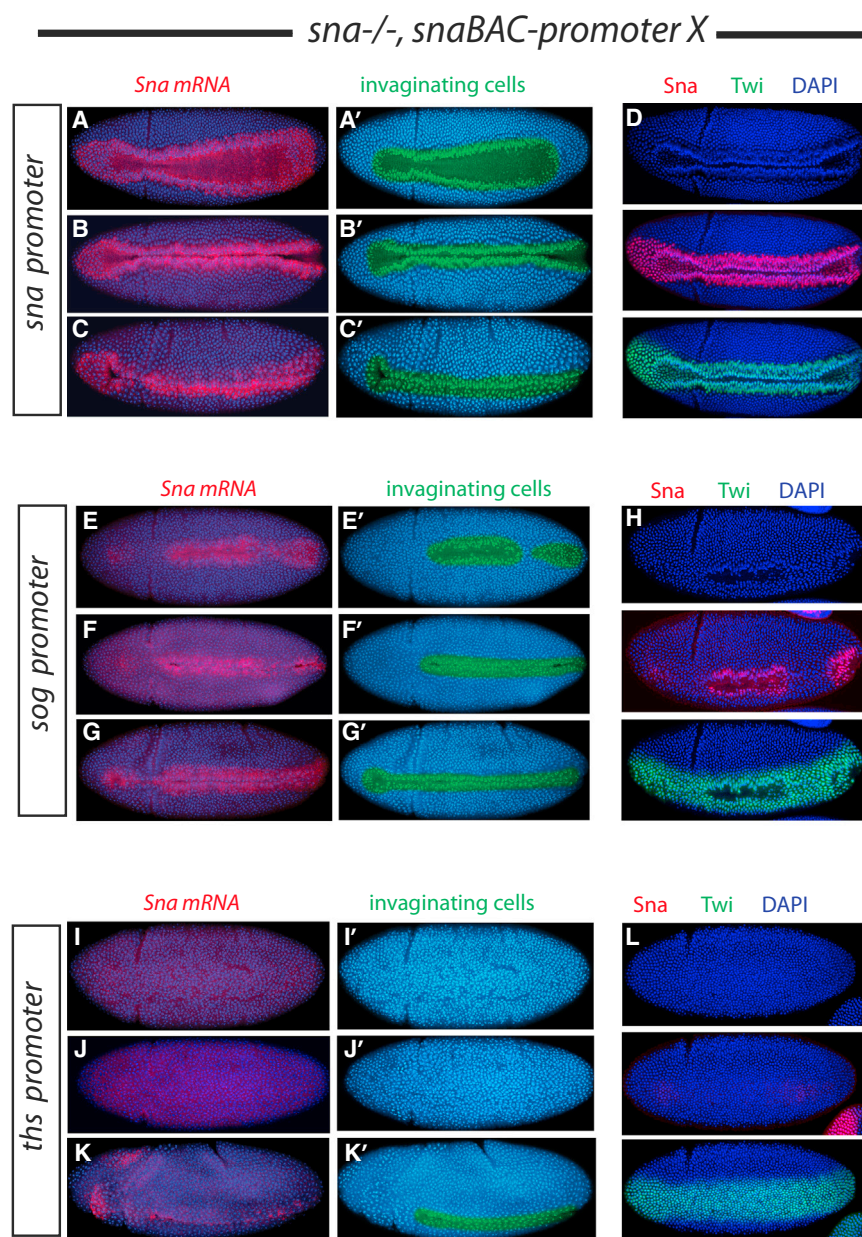


Figure 5. Stochastic Expression of *sna* Results in Gastrulation Defects

(A–L) Transgenic rescue embryos stained with a *sna* probe (in red) at gastrulation stages (A–C, E–G, and I–K) and correspondent invaginating cells false colored in green (A'–C', E'–G', and I'–K').

(A–C) When *sna* expression is driven by a *sna*BAC-*sna* promoter lacking the primary enhancer, all embryos gastrulate normally.

(E–G) Variable gastrulation defects are obtained when the *sna* promoter is replaced by the moderately paused *sog* promoter. Most embryos show pockets of ingressing cells (E and E'), and “half furrow” (F and F') and occasional embryos show a normal furrow (G and G').

(I–K) When *sna* is artificially depaused by replacing its promoter by the *ths* promoter sequence, most embryos fail to gastrulate (I–J'), but rare embryos exhibit an extended groove of invaginating cells (K and K').

(D, H, and L) Transgenic embryos stained with *sna* (red) and twist (Twi; green) antibodies at gastrulation when the ventral furrow is invaginating. See also Figure S5.

6D), as seen for the native *sna* promoter (Figure 4I). However, slightly less coordinated patterns of activation (t50, 4–7 min), e.g., *sog* promoter (Figure 4H), produce highly variable ventral furrows (Figure 6E). As the coordination is further reduced (t50, 7–12 min) (Figure 6F), most simulations show a complete loss of the furrow, although a small fraction of simulations produce half furrows in the posterior half of the embryo, as seen for the *ths* promoter (Figures 4G and 5K).

The bistable, all or none invagination of the anterior mesoderm can be explained by the combination of reduced levels of the Dorsal gradient, variable activation of the Snail repressor, and delayed synthesis of critical threshold levels of the Snail repressor (Figures 6E and 6F). The key insight from these simulations is that

nuclear gradient (Kanodia et al., 2009, 2011; Liberman et al., 2009; Reeves et al., 2012), which revealed a slight narrowing of the gradient in anterior regions. Our model also invokes *sna* autoregulation, which is suggested by the rapid loss of *sna* transcripts (Hemavathy et al., 1997) and *yellow* transcripts from a *sna* BAC transgene (Figures S5G–S5J) in *sna*^{-/-}/*sna*⁻ null embryos. We explored different mechanisms of autoregulation and obtained the most faithful results with an indirect model, whereby Snail represses a localized ectodermal repressor via a double-negative feedback loop (see Supplemental Information; Figure S6).

Computational simulations consistently produce uniform ventral furrows when the onset of *sna* expression is rapid and uniform (t50, 0–4 min after the onset of cc14) (Figures 6C and

short-range diffusion among neighboring nuclei can produce sufficient levels of Snail repressor to rescue small but not large patches of *sna*-expressing nuclei. The decision to maintain or repress *sna* expression occurs during a very tight time window, ~10–20 min after the onset of gastrulation. The key parameter underlying bistability is the time to synchrony because similar results are obtained when computer simulations are performed with a range of Hill coefficients for *sna* regulation and different diffusion rates for the Snail protein (see Figure S7).

DISCUSSION

Through a combination of BAC transgenesis, whole-genome ChIP assays, quantitative imaging, and computational modeling,

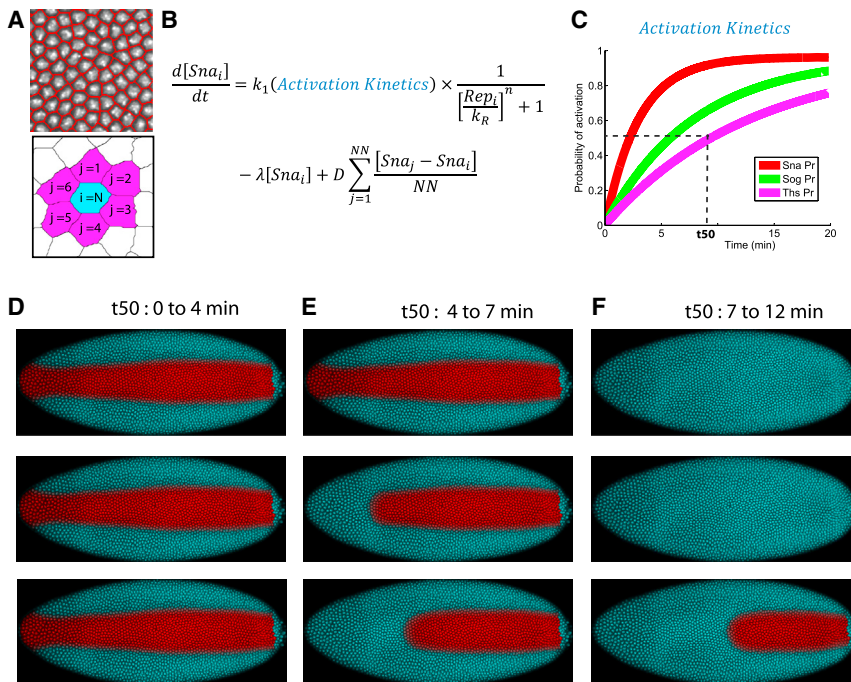


Figure 6. Modeling Gastrulation Variability: The Importance of Coordination

(A) Mesodermal region of a DAPI-stained embryo to show the segmentation process of the nuclei. The panel below is a schematic illustrating the neighbors (j) of a given mesodermal nucleus (i). We allow for nearest neighbor diffusion, where the “ i ” nucleus is diffusively coupled to its nearest neighbors that share a boundary (j , 1:6 in this case).

(B) Simplified mathematical model for Snail dynamic expression in a given nucleus (i). The key parameters are the timing of *sna* activation in the particular nuclei, the concentration of the neurogenic repressor (Rep), and the concentration of activators like Dorsal (k_1), number of nearest neighbors (NN), and the strength of the diffusive coupling between nuclei (D).

(C) Activation curves computationally obtained for three different promoters: *sna*, *sog*, and *ths*.

(D–F) Results of computational simulations when *sna* temporal coordination is affected; t_{50} values are indicated.

See also Figures S5, S6, and S7.

we obtained evidence that the time to synchrony is a critical determinant of coordinate cell behavior in the *Drosophila* embryo. Genes containing high levels of paused Pol II are activated in a more rapid and coordinated fashion than those containing intermediate or low levels. It is conceivable that paused Pol II will prove to be an essential feature of other patterning processes requiring rapid coordination of gene expression and cell behavior. For example, pausing of Notch signaling components (e.g., *Hes*) might help coordinate expression of the “clock” genes underlying somitogenesis in vertebrate embryos (Saga, 2012), which occurs on a timescale similar to mesoderm specification and invagination in *Drosophila* (~90 min from the onset of *sna* transcription to the formation of the ventral furrow).

Model for the Developmental Timing of Gene Activation

Recent studies in S2 cells suggest that developmentally regulated genes tend to contain either paused Pol II or inhibitory nucleosomes (Gilchrist et al., 2010). RNAi-mediated depletion of NELF led to reduced levels of paused Pol II and a concomitant increase in promoter-positioned nucleosomes. These studies prompted the proposal that paused Pol II might render genes poised for activation by excluding the formation of inhibitory nucleosomes at the core promoter.

It is possible that nonpaused genes mediate slow activation dynamics due to cell-cell variation in the eviction of inhibitory nucleosomes at the core promoter. If occupied by an inhibitory nucleosome, a distal enhancer will not be able to stimulate transcription as it engages the promoter. Either the enhancer must await repositioning or dynamic turnover of inhibitory nucleosomes to allow recruitment of Pol II. Either way, this process might be inherently stochastic, resulting in cell-to-cell variations in the onset of transcription.

In principle, this model can account for the spectrum of activation profiles seen for genes containing different levels of paused Pol II. A gene containing high levels, such as *tup*, is more likely to contain Pol II than an inhibitory nucleosome in a given cell at a given time as compared with genes containing little or no paused Pol II (e.g., *ths* and *pnr*, respectively). Consequently, upon induction, strongly paused genes exhibit synchronous patterns of activation because most of the promoters in the different cells of a tissue contain Pol II. In contrast, genes containing little or no paused Pol II are more likely to contain an inhibitory nucleosome in a given cell at a given time, resulting in variable delays in the onset of gene expression. Thus, the ratio of poised and inhibited states might determine the time to synchrony.

The *sna* gene contains lower levels of Pol II than the *tupPr* (Gaertner et al., 2012). When attached to the *pnrE*, it mediates a t_{50} activation profile of 24 min (Table 1), which is similar to the prototypic paused *hsp70* promoter but significantly slower than the *tupPr* (15 min) (see Figure 3). Recent studies in cultured cells suggest that transcription initiation can be dissociated from subsequent rounds of Pol II recruitment for p53 target genes, resulting in rapid rates of activation but low steady-state levels of mRNAs (Morachis et al., 2010). It has been suggested that strongly paused genes are not necessarily expressed at high levels due to the dwelling of Pol II within the proximal promoter at every round of transcription following activation (Gilchrist et al., 2012; Lin et al., 2011). This could reduce the rate of RNA synthesis by lowering the frequency of elongating Pol II complexes. In contrast, promoters containing weaker pausing elements might achieve higher loading of Pol II complexes due to shorter dwell times.

We propose that there is a “trade-off” between timing and levels of gene expression at paused genes. Genes containing

moderate levels of paused Pol II, such as *hsp70* and *sna*, might achieve an optimal balance between excluding inhibitory nucleosomes for synchronous activation and efficient loading of Pol II complexes. Evidence for this model is seen for the *tupPr*. It mediates rapid and synchronous activation of a *sna* BAC transgene but significantly weaker expression than the *sna* promoter (see [Figures S5K–S5M](#)).

Dynamic Control of the Dorsal-Ventral Patterning Network

The gene regulatory network underlying the spatial control of dorsal-ventral patterning has been extensively studied (reviewed by [Rushlow and Shvartsman, 2012](#)). Considerably less is known about the temporal dynamics of this process. Indeed, developmental timing has only recently become a critical focus of study, even in well-defined systems such as the patterning of the vertebrate neural tube ([Balaskas et al., 2012](#)). Here, we have shown that perturbing coordinate activation of the *sna* expression pattern leads to various invagination defects during gastrulation. Computational modeling ([Figure 6](#)) highlights the importance of timing in producing these defects. Delayed and asynchronous patterns of activation uncouple Snail from the other components of the dorsal-ventral patterning network, resulting in variable gaps and bistability of the ventral furrow, particularly in the anterior mesoderm. Indeed, this uncoupling results in the expression of high levels of the Dorsal and Twist activators in regions that fail to invaginate due to the delay in Snail expression (e.g., [Figures 5H and 5L](#)). This uncoupling of *sna* expression from its activators provides a vivid illustration of the importance of temporal dynamics in the control of complex developmental processes. A static gene network based on a simple Dorsal gradient affinity model does not appear to be sufficient to capture the intricacies of mesoderm morphogenesis.

The dorsal-ventral patterning network amplifies small changes in the levels of the dynamic Dorsal gradient to produce all or none patterns of *sna* expression. We believe that the key agent of this all or no bistable expression of Snail is the antirepression of competitive ectodermal repressors ([Hemavathy et al., 1997](#)). This indirect mechanism of Snail autoregulation may be the basis for producing the unusually sharp border of Snail expression at the boundary between the mesoderm and neurogenic ectoderm. This border determines whether cells become fully committed to EMT at gastrulation. Delays in coordinate *sna* expression are amplified by the dorsal-ventral patterning network to produce bistable gaps in the ventral furrow, particularly in anterior regions where there are slightly diminished levels of Dorsal nuclear transport.

Spectrum of Pausing and Cell Fate Decisions

Our results indicate that the continuum of Pol II pausing seen for different promoters leads to a continuum of temporal coordination in gene activation, spanning from highly stochastic to synchronous. As discussed above, synchronous activation of transcription is essential for coordinating mesoderm invagination; however, the stochastic regulation of gene expression is sometimes used to provide flexibility in cell fate specification within a tissue ([Eldar and Elowitz, 2010](#); [Losick and Desplan, 2008](#)). For example, stochastic specification mechanisms underlie fate

decisions in the *Drosophila* eye and human immune system ([Duffy et al., 2012](#); [Losick and Desplan, 2008](#)), whereby cells must adopt alternate fates to achieve a distribution of distinct functions. For example, there is a 70:30 distribution of alternative ommatidial identities in the eyes of higher Diptera that has been conserved for ~120 MYA ([Losick and Desplan, 2008](#)). Similarly, flexibility in the behavior of B lymphocytes is important for immune regulation ([Duffy et al., 2012](#)). Modulating the levels of paused Pol II could help tune the proportion of cells that adopt different fates through such stochastic specification mechanisms.

In summary, we have presented evidence that the promoter is a key agent for coordinating gene expression in the different cells of an embryonic tissue. Minimal promoter sequences are sufficient to establish paused Pol II and mediate synchronous patterns of gene expression. There is a tight correlation among the levels of paused Pol II, the time to synchrony, and the coordination of mesoderm invagination. We therefore propose that promoters ensure exquisite control of the complex cellular processes underlying morphogenesis.

EXPERIMENTAL PROCEDURES

Fly Genetics

The following fly lines were used for this study: *Sna* (BI3078), *NelF* (BI1569), *Spt5* (BI8352), *Trl* (*Trl^{FR67}*), and landing site line “VK33” (BI 24871). *Toll10b* is a maternal dominant gain-of-function mutation ([Schneider et al., 1991](#)); transgenes were introduced through the males. The genetic procedure used for the *sna* BAC rescue experiments was performed as described previously by [Perry et al. \(2010\)](#). For more details, see information in the [Extended Experimental Procedures](#).

Recombineering, Cloning, and Transgenesis

BAC recombineering was performed as described previously by [Venken et al. \(2006\)](#). The following CHORI BACs were used: *tup* BAC (84.8 kb, shortened to 60 kb) (CH321-68116); and *sna* BAC (CH322-18114-1). Sources of plasmid used and fly transgenesis using targeted integration are described in the [Extended Experimental Procedures](#) and [Table S3](#).

FISH and Quantitative Imaging Methods

FISH experiments were performed as described in [Bothma et al. \(2011\)](#). Embryos were imaged on a Carl Zeiss LSM 700 laser-scanning microscope, equipped with a motorized stage. Images were computationally segmented to localize nuclei and nascent transcripts of mRNA. More extensive details on the image analysis are included in the [Extended Experimental Procedures](#).

In order to measure the time to synchrony, activation curves were generated by quantifying the number of nuclei exhibiting nascent transcripts for various embryos at various time points during cc14. By fitting a cumulative gamma distribution, the t50 parameter was evaluated. Detailed description of this assay is provided in the [Extended Experimental Procedures](#).

Pol II ChIP-Seq

Pol II ChIP has been performed as described in [Zeitlinger et al. \(2007\)](#) using a Pol II antibody (CTD4H8; Millipore). Methods employed for library generation and ChIP-seq analysis are detailed in the [Extended Experimental Procedures](#).

Modeling

A detailed description of the mathematical model used to predict the evolution of the Snail protein is provided in the [Extended Experimental Procedures](#). Briefly, ordinary differential equations were used with the following key parameters: the timing of Snail activation, the concentration of a repressor and that of an activator (Dorsal), the number of nearest neighbors, and the diffusion between nuclei.

ACCESSION NUMBERS

All data have been submitted to the GEO under the accession number GSE36310.

SUPPLEMENTAL INFORMATION

Supplemental Information includes Extended Experimental Procedures, seven figures, and three tables and can be found with this article online at <http://dx.doi.org/10.1016/j.cell.2013.04.045>.

ACKNOWLEDGMENTS

The authors are grateful to Alistair Boettiger for sharing his ideas about Snail autoregulation. We also thank Mike Perry and Valerie Hilgers for their insightful discussions, Didier Rocancourt for help with artwork, and Lily Mirels and Eileen Wagner for comments on the manuscript. M.L. is the recipient of a Human Frontier fellowship. This work was funded by grants from the NIH, GM46638 to M.S.L. and GM47477 to D.S.G. M.L. and J.P.B. initiated efforts to create a stochastic pattern of *snail* activation. They also worked closely to determine activation profiles of both endogenous genes and transgenes containing minimal promoter sequences. J.P.B. conceived the use of *esg* as a means for identifying *sna*⁻/*sna*⁻ mutant embryos. M.L. worked with L.S. and D.S.G. to document the sufficiency of minimal promoter sequences in establishing paused RNA polymerase II via permanganate protection assays. She also worked with E.E., K.C., J.J., and J.Z. to document the spectrum of Pol II binding at different promoters via whole-genome ChIP-seq assays. J.P.B. performed the imaging and developed the segmentation algorithms needed to determine t50 activation profiles. He also performed imaging to count mRNAs and analyzed the models exploring the relationship between timing and levels of gene expression. J.P.B. modeled the dynamics of Snail protein expression. M.L. and E.E. designed and created minigenes and BAC transgenes. M.L. performed the genetic crosses. C.T. injected all the plasmid transgenes, and BestGene injected all the BAC transgenes. S.N. helped M.L. and J.P.B. to collect and stain embryos. M.L., J.P.B., and M.S.L. wrote the manuscript.

Received: October 4, 2012

Revised: February 23, 2013

Accepted: April 22, 2013

Published: May 23, 2013

REFERENCES

- Adelman, K., and Lis, J.T. (2012). Promoter-proximal pausing of RNA polymerase II: emerging roles in metazoans. *Nat. Rev. Genet.* *13*, 720–731.
- Ashe, H.L., Mannervik, M., and Levine, M. (2000). Dpp signaling thresholds in the dorsal ectoderm of the *Drosophila* embryo. *Development* *127*, 3305–3312.
- Balaskas, N., Ribeiro, A., Panovska, J., Dessaud, E., Sasai, N., Page, K.M., Briscoe, J., and Ribes, V. (2012). Gene regulatory logic for reading the Sonic Hedgehog signaling gradient in the vertebrate neural tube. *Cell* *148*, 273–284.
- Boehm, A.K., Saunders, A., Werner, J., and Lis, J.T. (2003). Transcription factor and polymerase recruitment, modification, and movement on dhsp70 in vivo in the minutes following heat shock. *Mol. Cell. Biol.* *23*, 7628–7637.
- Boettiger, A.N., and Levine, M. (2009). Synchronous and stochastic patterns of gene activation in the *Drosophila* embryo. *Science* *325*, 471–473.
- Boettiger, A.N., and Levine, M. (2013). Rapid transcription fosters coordinate snail expression in the *Drosophila* embryo. *Cell Rep* *3*, 8–15.
- Bothma, J.P., Magliocco, J., and Levine, M. (2011). The snail repressor inhibits release, not elongation, of paused Pol II in the *Drosophila* embryo. *Curr. Biol.* *21*, 1571–1577.
- Chen, H., Xu, Z., Mei, C., Yu, D., and Small, S. (2012). A system of repressor gradients spatially organizes the boundaries of Bicoid-dependent target genes. *Cell* *149*, 618–629.
- Duffy, K.R., Wellard, C.J., Markham, J.F., Zhou, J.H., Holmberg, R., Hawkins, E.D., Hasbold, J., Dowling, M.R., and Hodgkin, P.D. (2012). Activation-induced B cell fates are selected by intracellular stochastic competition. *Science* *335*, 338–341.
- Dunipace, L., Ozdemir, A., and Stathopoulos, A. (2011). Complex interactions between cis-regulatory modules in native conformation are critical for *Drosophila* snail expression. *Development* *138*, 4075–4084.
- Eldar, A., and Elowitz, M.B. (2010). Functional roles for noise in genetic circuits. *Nature* *467*, 167–173.
- Fay, A., Misulovin, Z., Li, J., Schaaf, C.A., Gause, M., Gilmour, D.S., and Dorsett, D. (2011). Cohesin selectively binds and regulates genes with paused RNA polymerase. *Curr. Biol.* *21*, 1624–1634.
- Gaertner, B., Johnston, J., Chen, K., Wallaschek, N., Paulson, A., Garruss, A.S., Gaudenz, K., De Kumar, B., Krumlauf, R., and Zeitlinger, J. (2012). Poised RNA polymerase II changes over developmental time and prepares genes for future expression. *Cell Rep.* *2*, 1670–1683.
- Gilchrist, D.A., Dos Santos, G., Fargo, D.C., Xie, B., Gao, Y., Li, L., and Adelman, K. (2010). Pausing of RNA polymerase II disrupts DNA-specified nucleosome organization to enable precise gene regulation. *Cell* *143*, 540–551.
- Gilchrist, D.A., Fromm, G., dos Santos, G., Pham, L.N., McDaniel, I.E., Burkholder, A., Fargo, D.C., and Adelman, K. (2012). Regulating the regulators: the pervasive effects of Pol II pausing on stimulus-responsive gene networks. *Genes Dev.* *26*, 933–944.
- Guenther, M.G., and Young, R.A. (2012). Grounded: transcriptional pausing in naive mESCs. *Cell Stem Cell* *10*, 484–485.
- Hemavathy, K., Meng, X., and Ip, Y.T. (1997). Differential regulation of gastrulation and neuroectodermal gene expression by Snail in the *Drosophila* embryo. *Development* *124*, 3683–3691.
- Hendrix, D.A., Hong, J.W., Zeitlinger, J., Rokhsar, D.S., and Levine, M.S. (2008). Promoter elements associated with RNA Pol II stalling in the *Drosophila* embryo. *Proc. Natl. Acad. Sci. USA* *105*, 7762–7767.
- Juven-Gershon, T., and Kadonaga, J.T. (2010). Regulation of gene expression via the core promoter and the basal transcriptional machinery. *Dev. Biol.* *339*, 225–229.
- Kalmar, T., Lim, C., Hayward, P., Muñoz-Descalzo, S., Nichols, J., Garcia-Ojalvo, J., and Martinez Arias, A. (2009). Regulated fluctuations in nanog expression mediate cell fate decisions in embryonic stem cells. *PLoS Biol.* *7*, e1000149.
- Kanodia, J.S., Rikhy, R., Kim, Y., Lund, V.K., DeLotto, R., Lippincott-Schwartz, J., and Shvartsman, S.Y. (2009). Dynamics of the Dorsal morphogen gradient. *Proc. Natl. Acad. Sci. USA* *106*, 21707–21712.
- Kanodia, J.S., Kim, Y., Tomer, R., Khan, Z., Chung, K., Storey, J.D., Lu, H., Keller, P.J., and Shvartsman, S.Y. (2011). A computational statistics approach for estimating the spatial range of morphogen gradients. *Development* *138*, 4867–4874.
- Kosman, D., Ip, Y.T., Levine, M., and Arora, K. (1991). Establishment of the mesoderm-neuroectoderm boundary in the *Drosophila* embryo. *Science* *254*, 118–122.
- Lee, H., Kraus, K.W., Wolfner, M.F., and Lis, J.T. (1992). DNA sequence requirements for generating paused polymerase at the start of hsp70. *Genes Dev.* *6*, 284–295.
- Lee, C., Li, X., Hechmer, A., Eisen, M., Biggin, M.D., Venters, B.J., Jiang, C., Li, J., Pugh, B.F., and Gilmour, D.S. (2008). NELF and GAGA factor are linked to promoter-proximal pausing at many genes in *Drosophila*. *Mol. Cell. Biol.* *28*, 3290–3300.
- Leptin, M. (2005). Gastrulation movements: the logic and the nuts and bolts. *Dev. Cell* *8*, 305–320.
- Levine, M. (2011). Paused RNA polymerase II as a developmental checkpoint. *Cell* *145*, 502–511.
- Leptin, M., and Grunewald, B. (1990). Cell shape changes during gastrulation in *Drosophila*. *Development* *110*, 73–84.
- Li, J., and Gilmour, D.S. (2011). Promoter proximal pausing and the control of gene expression. *Curr. Opin. Genet. Dev.* *21*, 231–235.

- Lieberman, L.M., Reeves, G.T., and Stathopoulos, A. (2009). Quantitative imaging of the Dorsal nuclear gradient reveals limitations to threshold-dependent patterning in *Drosophila*. *Proc. Natl. Acad. Sci. USA* *106*, 22317–22322.
- Lin, C., Garrett, A.S., De Kumar, B., Smith, E.R., Gogol, M., Seidel, C., Krumlauf, R., and Shilatifard, A. (2011). Dynamic transcriptional events in embryonic stem cells mediated by the super elongation complex (SEC). *Genes Dev.* *25*, 1486–1498.
- Losick, R., and Desplan, C. (2008). Stochasticity and cell fate. *Science* *320*, 65–68.
- Morachis, J.M., Murawsky, C.M., and Emerson, B.M. (2010). Regulation of the p53 transcriptional response by structurally diverse core promoters. *Genes Dev.* *24*, 135–147.
- Nichols, J., and Smith, A. (2011). The origin and identity of embryonic stem cells. *Development* *138*, 3–8.
- Ong, C.T., and Corces, V.G. (2011). Enhancer function: new insights into the regulation of tissue-specific gene expression. *Nat. Rev. Genet.* *12*, 283–293.
- Perry, M.W., Boettiger, A.N., Bothma, J.P., and Levine, M. (2010). Shadow enhancers foster robustness of *Drosophila* gastrulation. *Curr. Biol.* *20*, 1562–1567.
- Reeves, G.T., Trisnadi, N., Truong, T.V., Nahmad, M., Katz, S., and Stathopoulos, A. (2012). Dorsal-ventral gene expression in the *Drosophila* embryo reflects the dynamics and precision of the dorsal nuclear gradient. *Dev. Cell* *22*, 544–557.
- Rushlow, C.A., and Shvartsman, S.Y. (2012). Temporal dynamics, spatial range, and transcriptional interpretation of the Dorsal morphogen gradient. *Curr. Opin. Genet. Dev.* *22*, 542–546.
- Saga, Y. (2012). The synchrony and cyclicity of developmental events. *Cold Spring Harb. Perspect. Biol.* *4*, a008201.
- Schneider, D.S., Hudson, K.L., Lin, T.Y., and Anderson, K.V. (1991). Dominant and recessive mutations define functional domains of Toll, a transmembrane protein required for dorsal-ventral polarity in the *Drosophila* embryo. *Genes Dev.* *5*, 797–807.
- Schuettengruber, B., Ganapathi, M., Leblanc, B., Portoso, M., Jaschek, R., Tolhuis, B., van Lohuizen, M., Tanay, A., and Cavalli, G. (2009). Functional anatomy of polycomb and trithorax chromatin landscapes in *Drosophila* embryos. *PLoS Biol.* *7*, e13.
- Shopland, L.S., Hirayoshi, K., Fernandes, M., and Lis, J.T. (1995). HSF access to heat shock elements in vivo depends critically on promoter architecture defined by GAGA factor, TFIID, and RNA polymerase II binding sites. *Genes Dev.* *9*, 2756–2769.
- Sweeton, D., Parks, S., Costa, M., and Wieschaus, E. (1991). Gastrulation in *Drosophila*: the formation of the ventral furrow and posterior midgut invaginations. *Development* *112*, 775–789.
- Venken, K.J., He, Y., Hoskins, R.A., and Bellen, H.J. (2006). P[acman]: a BAC transgenic platform for targeted insertion of large DNA fragments in *D. melanogaster*. *Science* *314*, 1747–1751.
- Vincent, S.D., and Buckingham, M.E. (2010). How to make a heart: the origin and regulation of cardiac progenitor cells. *Curr. Top. Dev. Biol.* *90*, 1–41.
- Zeitlinger, J., Stark, A., Kellis, M., Hong, J.W., Nechaev, S., Adelman, K., Levine, M., and Young, R.A. (2007). RNA polymerase stalling at developmental control genes in the *Drosophila melanogaster* embryo. *Nat. Genet.* *39*, 1512–1516.